Optical properties of the $(CuInSe_2)_{1-x}$-$(2ZnSe)_x$ system*

J. N. Gan and J. Tauc†
Department of Physics and Division of Engineering, Brown University, Providence, Rhode Island 02912

V. G. Lambrecht, Jr. and M. Robbins
Bell Laboratories, Murray Hill, New Jersey 07974

(Received 18 August 1975)

Optical electronic transitions were studied in the $(CuInSe_2)_{1-x}$-$(2ZnSe)_x$ system from 0.5 to 14 eV. The system crystallizes in the chalcopyrite structure for $x \leq 0.43$ and in the zinc-blende structure for $x \geq 0.48$. The absorption edge was found to be direct for all the compositions and the energy gap varies with x parabolically, without discontinuity at the structural transition. This dependence is associated with the substitutional disorder in the mixtures. Reflection measurements showed substantial differences between the compositions with the chalcopyrite structure and those with the zinc-blende structure. The additional peaks observed for the compounds with the chalcopyrite structure are ascribed to pseudodirect transitions which become allowed by zone folding. The optical constants in the visible and ultraviolet regions were determined from the reflection spectra by Kramers-Kronig analysis. The dependence of the absorption bands on composition and structure is discussed and possible assignments are suggested. The effective number of electrons per atom contributing, in the energy range studied, to optical transitions was calculated and was found to depend strongly on the amount of Cu d electrons in the mixture as well as on the crystal structure.

INTRODUCTION

Ternary compounds of the form II-IV-V_2 and I-III-VI_2 which have the chalcopyrite structure are analogs of the binary III-V and II-VI semiconductors, respectively. Studies of the electronic properties of these materials have been reviewed recently by Shay and Wernick.[1] Because they have similar structures and the same number of valence electrons per atom, one would expect the optical spectra and electronic band structure to be closely related to the binary analogs. This is indeed the case for the II-IV-V_2 compounds.[1] The I-III-VI_2 compounds are, however, less well understood. A serious complication is associated with strong d-level interaction. The core d-levels of the group-I atoms are close in energy to the outer electron states and in the ternary compounds, they are found in the valence bands.[2,3] As a consequence, the direct energy gaps observed in the I-III-VI_2 compounds are smaller than the gaps in the II-VI analogs by amounts up to 1.6 eV, and the spin-orbit splittings observed in the ternary compounds are small relative to the values observed in the binary analogs.[1]

In order to study the effects of the d-levels as well as of the structural change on the band structure, we measured the transmission (close to the absorption edge) and the reflection spectra (0.5–14 eV) of solid solutions of a ternary compound ($CuInSe_2$) with its binary analog (ZnSe). The system crystallizes in the chalcopyrite structure when the ternary compound prevails and in the zinc-blende structure for large concentrations of ZnSe. This gave us a convenient system to see how gradual additions of the group-I atoms as well as how a structural change from the zinc-blende to the chalcopyrite form may change the band structure. However, $CuInSe_2$ is not isoelectronic with ZnSe. We chose this ternary compound rather than the isoelectronic $CuGaSe_2$ because it was much easier to prepare good single crystals.

SAMPLES

The system $(CuInSe_2)_{1-x}$ - $(2ZnSe)_x$ has the chalcopyrite structure for $x \leq 0.43$ and the zinc blende structure for $x \geq 0.48$. In the chalcopyrite structure, the Zn atoms randomly replace the Cu and the In atoms which remain ordered relative to each other. For the zinc-blende phase, the Cu and the In atoms are no longer ordered and replace the Zn atoms randomly. The c/a ratio for the chalcopyrite phase remains equal to 2 (± 1%) from $x = 0$ to $x = 0.43$, and the unit cell is very close to twice that of ZnSe.[4]

The zinc-blende structure has the point group T_d^2 while the chalcopyrite structure belongs to the point group D_{2d}. The character tables are published in Ref. 5 and 6.

Single crystals with compositions $x = 0$, 0.08, 0.21, 0.33, 0.43, 0.48, and 0.6 were prepared by directional freezing in horizontal boats or by the Bridgman method. Details about the preparation techniques have been described previously.[4] Samples of good crystallinity were selected and oriented using back-reflection Laue x-ray photographs. For our experiments, we obtained two orientations of samples for each composition (one with the c axis on the plane of the surface and the other with the c axis perpendicular to the surface). The samples were first ground on glass with 1200-mesh Buehler grinding compound. After this, we

polished the samples with Linde 0.3 μm alumina abrasives on a felt pad. Finally, the samples were polished and etched with Syton. Clear, specular surfaces with few scratches were obtained.

EXPERIMENTAL TECHNIQUES

The transmission T was measured with a Cary 14 spectrometer at room temperature near the absorption edge (which ranges from 1.02 to 2.8 eV) on samples with two different thicknesses (d_1 and d_2). The absorption coefficient was then calculated from the formula $\alpha = (d_2 - d_1)^{-1} \ln T_1/T_2$.

In the reflectivity measurements, the rotating-light-pipe method[7] was used. A bent quartz pipe was rotated at 40 Hertz to collect the incident beam and the reflected beam from the sample. This is shown in Fig. 1 with the associated signal processing electronics.

The light coming out of the other end of the light pipe is detected by a photomultiplier and gives electrical pulses proportional to the incident beam intensity (I_0) and the reflected beam intensity (R_0). The base line of the pulses is proportional to the dark current (D) of the photomultiplier. These pulses are passed through a multichannel box-car integrator to obtain the signals I_0-D and R_0-D. A Kepco programmable power supply was used to control the photomultiplier voltage so that I_0-D is constant as the wavelength of the incident light is changed. This gave us the absolute reflectivity $R = (R_0 - D)/(I_0 - D)$.

In the near-ultraviolet, visible, and near-infrared regions (0.5–6.2 eV), we used a Perkin-Elmer Model E-14 monochromator. In this region, the precision of the absolute reflectivity measurement is limited by the difference between a converging incident beam and a divergent reflected beam.

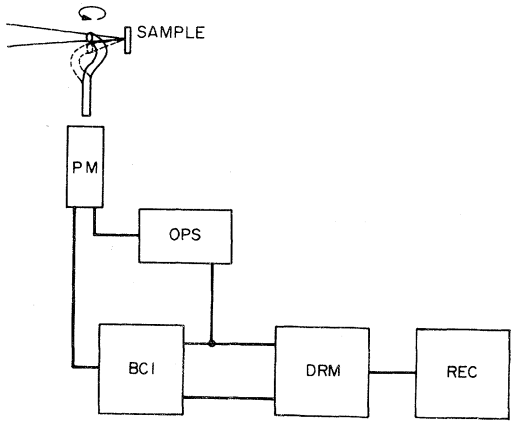

FIG. 1. Rotating light pipe and signal processing electronics. PM, photomultiplier; OPS, operational power supply; BCI, box-car integrator; DRM, digital ratio meter: REC, recorder.

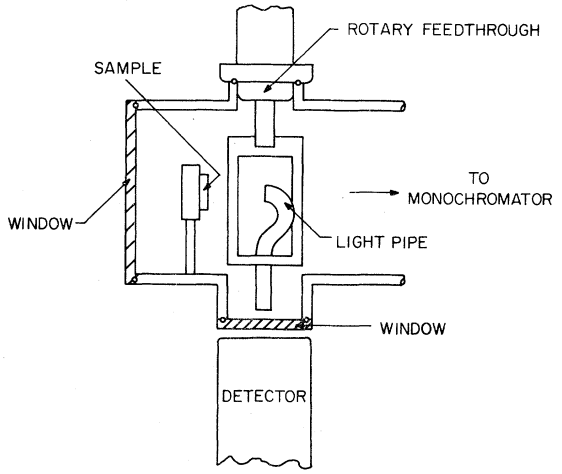

FIG. 2. Sample chamber used for reflectivity measurements in the vacuum uv region.

These two beams enter the light pipe at different angles and are transmitted differently. Improvement was obtained by making the surface of the incident end of the light pipe rough. Comparison of this technique with other absolute reflectivity measurements indicate an accuracy within 5%. However, relative changes in reflectivity smaller than 0.2% can be detected.

In the vacuum ultraviolet region (5–14 eV), we used a McPherson Model 231 vacuum uv monochromator. A sample chamber was built for the sample and the light pipe assembly is shown in Fig. 2. A Ferrofluidics magnetic rotary feedthrough enabled us to obtain up to 10^{-6} Torr in the main chamber even when the shaft was rotated at 40 Hz.

The front end of the light pipe was sprayed uniformly with sodium-salicylate phosphor to convert ultraviolet radiation into visible light. An EMI S-11 photomultiplier was then used to detect the visible light. Maximum response was obtained for a coating thickness of about 1000 Å. A uniform thickness on the front face of the light pipe was obtained by blowing N_2 gas on a tapered glass tube dipped in a saturated solution of sodium salicylate in distilled water. The light pipe was held by hand and moved several times through the spray. For the light source, we modified a McPherson Model 630 Hinteregger discharge lamp for hot-cathode operation.[8] Two holes were drilled through the cathode plate for high-voltage feedthroughs. A thoriated tungsten wire (0.23 in. dia) was wound into a coil and connected to the feedthroughs. The power source for the discharge consisted of a Sorensen Model DCR 600-2.4 high-voltage supply. The filament was heated by a dc power supply. We found a good operating condition for a main chamber pressure of about 2×10^{-4} Torr and a

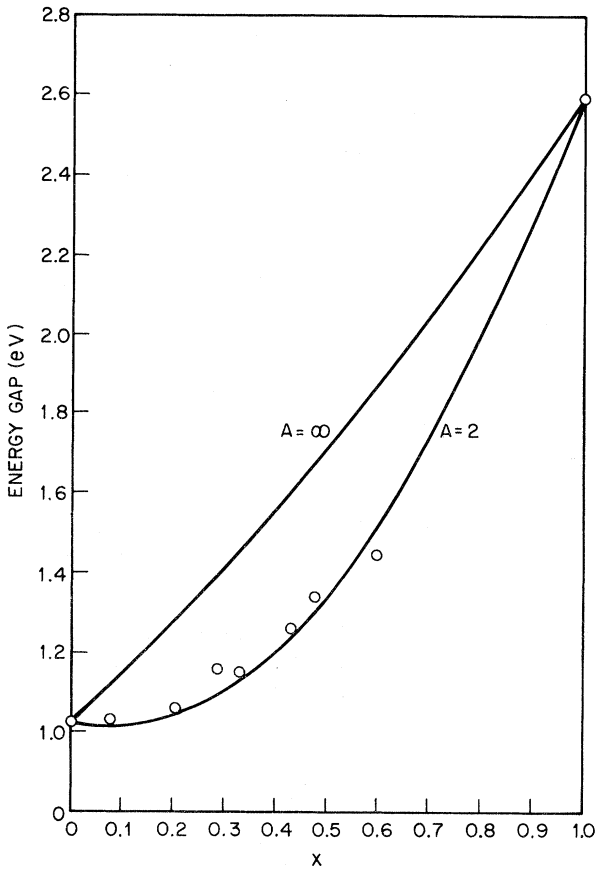

Fig. 3. Calculated energy gap compared with the experimental points.

discharge current of about 1.5 a. The filament current was held at about 20 a. The power of the lamp was about 200 w.

The hot-cathode operation enabled us to obtain light intensity more than ten times of what we had with the cold-cathode discharge. The lamp was operated without a window so that H_2 gas flowed into the main chamber. This allowed us to obtain photon energies up to 14 eV.

RESULTS AND DISCUSSION

Absorption edge

The absorption coefficients were determined in the range from $\alpha \simeq 3$ to $\alpha \simeq 180$ cm^{-1} and were found to fit a relation of the form $\alpha \sim (\hbar\omega - E_g)^{1/2}$, indicating direct energy gaps, for all the compositions. Extrapolation of the α-vs-$\hbar\omega$ curves gave us values for the energy gap E_g. No difference in the transmission was observed for light polarized perpendicular and parallel to the c axis of the chalcopyrite compounds. This is probably due to the c/a ratio being equal to 2. In some samples, we observed absorption edges which were broadened, presumably by structural imperfections and impurities similarly, as reported by Shay *et al.*[9] However, these samples were discarded. The good samples had sharp absorption edges ($\Delta\alpha/\Delta E \simeq 6\times10^3$ cm^{-1} eV^{-1}).

The energy gap versus composition is shown in Fig. 3. We found no discontinuity near the structural change which occurs between $x = 0.43$ and 0.48.

The parabolic dependence of the energy gap on the composition of the alloy can be explained by disorder effects. The variation of the energy gap of several semiconductor alloys versus composition can be fitted by an equation given by Van Vechten[10–13]:

$$E_0 = [E_{0,h} - (D-1)\Delta E_0][1 + (C/E_{0,h})^2]^{1/2} + x(x-1)[C(2) - C(1)]^2/A,$$

where the first term is due to the variation of the virtual-crystal potential and the second term is due to the aperiodic potential term from disorder effects. $E_{0,h}$ is the contribution to E_0 from the symmetric part and C is the contribution from the antisymmetric part of the virtual-crystal potential.[14] The factor $(D-1)\Delta E_0$ (where $D \simeq n_{eff}$, n_{eff} is the effective number of contributing electrons per atom) is introduced to take into account contributions from core levels. A is an energy determined by the best fit to experimental data. The parameters $E_{0,h}$, D, ΔE_0, and C are dependent on the composition and we assumed this dependence to be linear. The best fit to experimental data was found for $A = 2$ eV. This is shown in Fig. 3 with and without the disorder term ($A = \infty$ for the latter case). One observes that the effect of the disorder term is to lower the energy gap from a linear dependence on composition. The effect seems to be greatest near the structural change which occurs between $x = 0.43$ and 0.48. This is to be expected as the greatest disorder should occur there.

Interband transitions above the edge

The reflectivity measurements in the range 0.5–14 eV are shown in Fig. 4. Again, we did not observe any polarization dependence in the chalcopyrite compounds. The upper five curves correspond to the chalcopyrite phase and the lower three curves correspond to the zinc-blende phase. Structures found[15] in ϵ_2 are plotted as a function of composition in Fig. 5. A simple model of the energy band of $CuInSe_2$ may be obtained by folding the energy bands of ZnSe into a chalcopyrite Brillouin zone. This is shown in Fig. 6. The structure labeled D' near 3 eV was observed only for the compounds with the chalcopyrite structure and may be associated with transitions from the top of the valence band to a state which maps into the center of the chalcopyrite Brillouin zone by

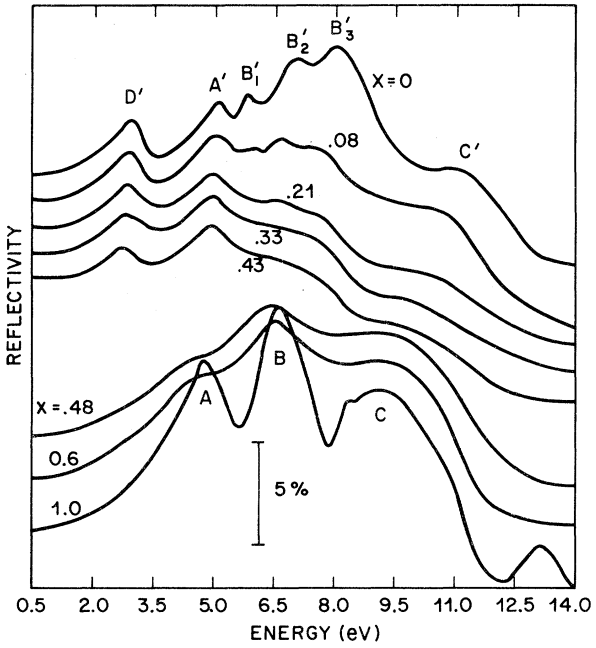

FIG. 4. Reflectivity of the $(CuInSe_2)_{1-x}$-$(2ZnSe)_x$ system. At 0.5 eV the measured reflectivities were: 25.7% (for $x=0$), 25.2% (0.08), 25.0% (0.21), 24.8% (0.33), 24.3% (0.43), 23.8% (0.48), 22.0% (0.60), 18.0% (1.00).

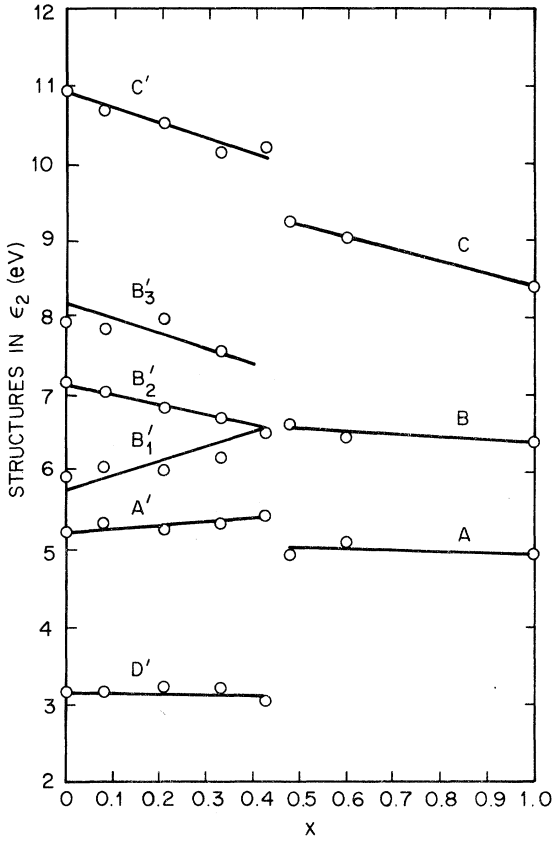

FIG. 5. Structrues in ϵ_2 vs composition for the $(CuInSe_2)_{1-x}$-$(2ZnSe)_x$ system.

zone folding. A probable origin of this state is X_{1c} in ZnSe, which maps into Γ_2. The details of this assignment are discussed in Ref. 16.

In ZnSe, the structures A, B, and C were identified as due to the transitions $L_{3v} \rightarrow L_{1c}$, $X_{5v} \rightarrow X_{1c}$, and $L_{3v} \rightarrow L_{3c}$, respectively.[17,18] These structures shift continuously on admixture of $CuInSe_2$, indicating that the main features of the energy band remain the same. The broadening (see Fig. 4) probably occurs because of the increase in disorder.

The energy of the structure A' appears to change little with composition and lies close in energy to A, suggesting that they may have the same origin. In the chalcopyrite Brillouin zone, L_{3v} maps into N_{1v} and L_{1c} maps into N_{1c}. The energy of the transition $N_{1v} \rightarrow N_{1c}$ should therefore remain close to the energy of the transition $L_{3v} \rightarrow L_{1c}$.

The structures B'_1, B'_2, and B'_3 merged into a shoulder as more ZnSe are added and lies close in energy to B. Possible origins of these transitions are: $X_5 \rightarrow X_1$ (at Γ), $X_5 \rightarrow X_1$ (at T), $\Gamma_{15} \rightarrow X_3$, $W_3 \rightarrow \Gamma_1$, $\Delta_5 \rightarrow \Delta_1$ (at T), and $\Sigma_2 \rightarrow \Sigma_1$ (at N).

More transitions are possible at higher energy, and the structure C' may correspond to $L_{3v} \rightarrow L_{3c}$ (at N) and other possible transitions. C' remains as a broad shoulder at $x=0$, indicating it may have contributions from many parts of the Brillouin zone.

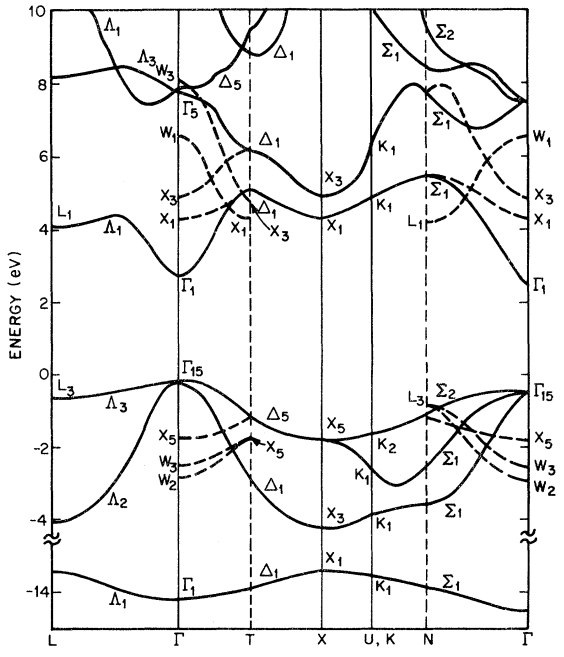

FIG. 6. Band structure of ZnSe folded into the chalcopyrite Brillouin zone.

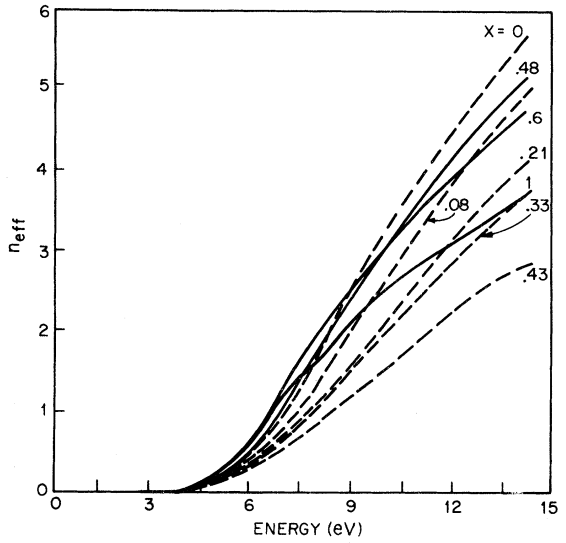

FIG. 7. Effective number of electrons per atom contributing up to energy E.

Effective electron concentration

The effective number of valence electrons per atom contributing to the optical properties in the range $0-\omega_0$ can be calculated from the equation[19]

$$n_{eff}(\omega_0) = \frac{m}{2\pi^2 N e^2} \int_0^{\omega_0} \omega \epsilon_2 \, d\omega \ .$$

From the $\epsilon_2(\omega)$ obtained from Kramers-Kronig analysis of the reflection measurements, we calculated $n_{eff}(\omega_0)$ for different compositions of the $(CuInSe_2)_{1-x}$-$(2ZnSe)_x$ system (see Fig. 7). The dotted and solid lines are for compositions with the chalcopyrite and the zinc-blende structures, respectively. If the valence band can be decoupled from the lower lying bands, n_{eff} should saturate at a value which corresponds to the electrons contributing from the valence bands.

For ZnSe, this saturation value is expected to be four. At our highest photon energy $\hbar\omega = 14$ eV, n_{eff} is 3.6. As $CuInSe_2$ is added, n_{eff} (14 eV) increases because we obtain contributions from the d bands of copper. An unexpected drop in n_{eff} occurs between $x = 0.48$ and 0.43 when the structure changes from zinc blende to chalcopyrite (Fig. 8). Within the chalcopyrite structure, n_{eff} (14 eV) increases with decreasing x, reaching a value of 5.7 in $CuInSe_2$. The expected saturation value of n_{eff} in $CuInSe_2$ is 6.5 electrons/atoms (Cu contributes one $4s$ electron plus ten $3d$ electrons, In two $5s$ electrons and one $5p$ electron, Se six $4s$ and $4p$ electrons).

The large change of n_{eff} at the phase transition is difficult to explain. It would indicate that in the chalcopyrite structure the valence-band electrons are spread over a considerably broader energy interval than in the zinc-blende structure. Perhaps this could be explained by a repulsive interaction of the d bands on states which map into the center of the Brillouin zone from the boundary of the zinc-blende Brillouin zone, so that the optical transitions are shifted beyond 14 eV. The effect, however, may rather be due to the differences in the surfaces of the samples. It is known that the condition of the surface affects the reflectivity in the uv region significantly.[20] Measurement of the Auger spectra of two samples of compositions near the structural transition ($x = 0.43$ and 0.48) showed large differences in the composition of the first 20-Å surface layers although the surfaces were prepared by identical procedures. This point deserves a detailed study.

ACKNOWLEDGMENTS

We would like to thank J. H. Wernick for his interest and encouragement in this work, J. C. Phillips, J. L. Shay, and S. R. Nagel for their helpful comments on the manuscript, and T. R. Kirst for the technical assistance. We are grateful to P. Estrup and G. Robertshaw for the Auger data. We also appreciate the advice of H. Fritzsche and G. W. Rubloff on the design of the light-pipe reflectometer.

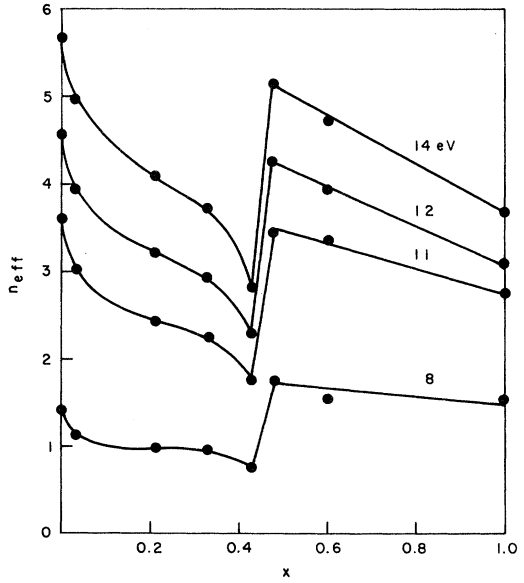

FIG. 8. Effective number of electrons per atom vs composition.

*Work at Brown University was supported in part by a grant from AROD (DA-ARO-D-31-124-72-G204) and also by the NSF through the general support of Materials Science at Brown University.

†Also at Bell Laboratories, Murray Hill, N.J. 07974.

[1]J. L. Shay and J. H. Wernick, *Ternary Chalcopyrite Semiconductors-Growth, Electronic Properties, and Applications* (Pergamon, New York, 1975).

[2]M. J. Luciano and C. J. Vesely, Appl. Phys. Lett. 23, 60 (1973).

[3]S. Kono and M. Okusawa, J. Phys. Soc. Jpn. 37, 1301 (1974).

[4]V. G. Lambrecht, Jr., Mater. Res. Bull. 8, 1383 (1973).

[5]R. H. Parmenter, Phys. Rev. 100, 573 (1955).

[6]Von R. Sandrock and J. Treusch, Z. Naturforsch. A 19, 844 (1964).

[7]G. W. Rubloff, H. Fritzsche, J. Gerhardt, and J. Freeouf, Rev. Sci. Instrum. 42, 1507 (1971).

[8]D. E. Eastman and J. J. Donelon, Rev. Sci. Instrum. 41, 1648 (1970).

[9]J. L. Shay, E. Buehler, and J. H. Wernick, Phys. Rev. B 4, 2482 (1971).

[10]J. A. Van Vechten and T. K. Bergstresser, Phys. Rev. B 1, 3351 (1970).

[11]J. A. Van Vechten, Phys. Rev. 182, 891 (1969).

[12]J. A. Van Vechten, Phys. Rev. 187, 1007 (1969).

[13]J. A. Van Vechten, Phys. Rev. B 7, 1479 (1973).

[14]J. C. Phillips, Phys. Rev. 166, 832 (1968).

[15]J. N. Gan, Ph.D. thesis (Brown University, 1975) (unpublished).

[16]J. N. Gan, J. Tauc, V. G. Lambrecht, Jr., and M. Robbins, Solid State Commun. 15, 605 (1974).

[17]M. Aven, D. T. F. Marple, and B. Segall, J. Appl. Phys. 32, 2261 (1961).

[18]J. Walter and M. L. Cohen, Phys. Rev. 183, 763 (1969).

[19]H. R. Philipp and H. Ehrenreich, Phys. Rev. 129, 1550 (1963).

[20]J. C. Phillips, Phys. Rev. B 9, 2775 (1974).